ORGANIC CHEMISTRY FRONTIERS

RESEARCH ARTICLE

View Article Online
View Journal | View Issue

Cite this: *Org. Chem. Front.*, 2026, **13**, 423

Novel antimicrobial self-assembled cyclic peptide nanotubes containing (1*R*,3*S*,4*R*,5*R*)-3-amino-4,5-dihydroxycyclohexane-1-carboxylic acid, a new building block for developing mimetics of saccharide–peptide hybrids

Eva González-Freire,[a] Marcos Vilela-Picos,[a] Verónica Prado,[a] Antonio Pérez-Estévez,[b] Rafael Seoane,[b] Manuel Amorín,*[a] Concepción González-Bello*[a] and Juan R. Granja*[a]

Received 1st October 2025,
Accepted 29th October 2025

DOI: 10.1039/d5qo01374g

rsc.li/frontiers-organic

A new class of supramolecular antimicrobials based on D,L-cyclic peptides containing a dihydroxylated-γ-residue, which was designed to mimic the saccharide component present in certain carbohydrate–peptide hybrids, is described. The fully protected amino acid was prepared from shikimic acid and incorporated into clickable amphipathic cyclic peptides. The resulting peptides self-assemble into nanotubes that interact with bacterial membranes, ultimately causing cell death. Notably, the incorporation of this new residue not only retains antimicrobial activity but also significantly reduces toxicity in mammalian cells, thereby broadening the therapeutic window of these peptides.

Introduction

One of the main medical and social challenges hindering the sustainable development of our society is the increasingly global spread of multidrug-resistant bacteria.[1] Despite the remarkable scientific and medical advances of the last century, during which most of the antibacterial agents were developed, significant ground has been lost in recent decades in this fight. According to the World Health Organization (WHO), bacterial resistance to antibiotics will be one of the three greatest threats to human health in the coming decades.[2] This discouraging situation is due both to the evolutionary and adaptive nature of bacteria,[3] which can develop and transfer resistance to existing drugs, and to the overuse and misuse of antibiotics over the years. This challenge is compounded by the difficulties involved in developing new drugs with alternative mechanisms of action.[4] Over the last 20 years, only a few new antibacterial drugs have been approved, and resistant bacterial strains have emerged and spread shortly after their use. In this respect, antimicrobial peptides (AMPs), which are naturally present in pluricellular organisms, constitute the first defence barrier against bacteria.[5] These peptides have existed in nature for thousands of years, yet resistance phenomena remain quite unusual.[6] The mechanism of action of these peptides is closely related to their structure. Although they may exhibit multiple modes of action, they preferentially target the bacterial cell membrane, disrupting the phospholipid bilayer and causing ion imbalance, which ultimately triggers bacterial death. Structurally, most of these peptides are amphipathic and cationic, features that facilitate their interaction with negatively charged bacterial membranes.

Antimicrobial self-assembled cyclic peptides (AMcPs) with a tubular shape are synthetic alternatives to AMPs with promising properties.[7] They behave as supramolecular medicines,[8,9] in which small units assemble under specific conditions into larger and ordered biologically active aggregates.[10–12] In recent years, the use of supramolecular nanomedicines has emerged as a novel therapeutic approach in which their dynamic behaviour, including their response to external stimuli, and the structural features derived from their shape and nanometric size are combined to obtain enhanced pharmacological profiles, greater selectivity and, in most cases, longer circulation times *in vivo*. In this case, the active antimicrobial form (peptide nanotubes) is generated directly on bacterial membranes, driven by electrostatic interactions with anionic phospholipids (Fig. 1a), which are abundant in bacterial

[a]*Centro Singular de Investigación en Química Biolóxica e Materiais Moleculares (CiQUS), Departamento de Química Orgánica, Universidade de Santiago de Compostela, Jenaro de la Fuente s/n, 15782 Santiago de Compostela, Spain. E-mail: manuel.amorin@usc.es, concepción.gonzalez.bello@usc.es, juanr.granja@usc.es*

[b]*Departamento de Microbiología y Parasitología, Facultad de Medicina, Universidade de Santiago de Compostela, 15782 Santiago de Compostela, Spain*

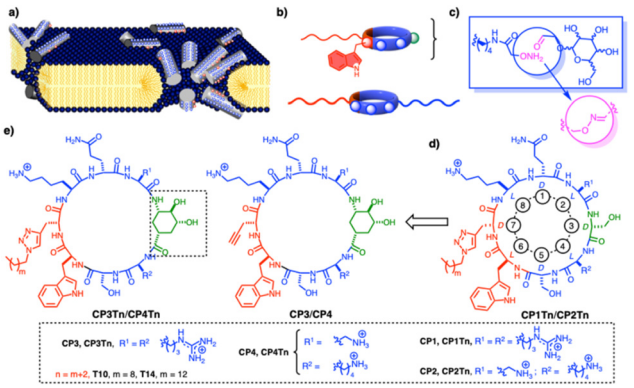

Fig. 1 New antimicrobial cyclic peptides: (a) proposed mode of action of AMcPs; (b) previous model of CPs modified with polymers (bottom) or alkyl chains (top); (c) precedent for the saccharide incorporation strategy;[17] (d) peptide model from which the derivatives studied in this work are derived; and (e) CPs developed in this work in which the (1*R*,3*S*,4*R*,5*R*)-3-amino-4,5-dihydroxycyclohexane-1-carboxylic acid moiety (**Dhγ**) in the targeted peptides is highlighted in green.

membranes.[13–16] Recently, we and others have further studied the antimicrobial properties of self-assembling cyclic peptides modified with polymers or alkyl triazole groups decorating the outer part of the peptide core (Fig. 1b).[13–17] To this end, we have developed a chemical approach based on two orthogonal click-type transformations to incorporate two different chemical components. This strategy demonstrated that the introduction of long alkyl chains attached to a triazole ring and saccharide moieties improves the antimicrobial properties of AMcPs. These chains reduce the number of hydrophobic residues needed to generate active amphipathic structures, resulting in an increase in the number of hydrophilic residues and thus improving their solubility in aqueous media. On the other hand, the saccharide moiety provides greater protection by decreasing cytotoxicity to mammalian cells (*i.e.* haemolysis) (Fig. 1c).[18]

Additionally, our group has extensively investigated self-assembled cyclic peptides containing γ-aminocycloalkanecarboxylic acids (γ-Aca), which exhibit better assembling properties than pristine D,L-α-CPs.[11] The main advantages of incorporating these γ-residues lie in their improved pre-organization for CP stacking and their strong preference for forming parallel β-sheet-type structures.[19–23] Although our studies have focused mainly on non-functionalized γ-Aca, we have also developed other more complex derivatives obtained from saccharides.[24,25] These modified residues have proven to be specially suitable for modulating the internal and external properties of the resulting supramolecular assemblies. In this regard, we envisage that the incorporation of polyhydroxylated cyclic γ-residues, such as those derived from glucuronic acid, could provide improved tolerance similar to that observed with saccharide-functionalized AMcPs,[26–28] creating a new class of peptidoglycan mimetics.[29] Unfortunately, CPs containing glucuronic acid derivatives exhibited limited stability in aqueous media, which prevented their use for this purpose.[28] The incorporation of these polyhydroxylated residues,[30] in addition to improving the solubility of the CPs, may also offer new ways of interacting with bacterial surfaces, improving their selectivity. Herein, we report an efficient synthesis of a dihydroxylated γ-Aca and explore the self-assembly and antibacterial properties of a new class of cyclic peptides incorporating this residue. The two hydroxyl groups of the γ-amino acid are exposed on the external surface of the nanotube, thereby modulating its physicochemical properties. Specifically, we proposed replacing one of the serine residues in biologically active CPs[17] with (1*R*,3*S*,4*R*,5*R*)-3-amino-4,5-dihydroxycyclohexane-1-carboxylic acid (**Dhγ**, Fig. 1). For this purpose, the synthesis of the fully protected γ-amino acid **6** and its subsequent incorporation into AMcPs are described. Considering the previous studies, we designed cationic amphipathic peptides, **CP3T*n*** and **CP4T*n*** (Fig. 1e), using **CP1T10** and **CP2T10**, two of the most potent antimicrobial peptides previously reported,[17] as references, or their corresponding precursors lacking the alkyl chain, **CP1** and **CP2** (Fig. 1d).[31] The designed CPs contain only two hydrophobic residues, a Trp and propargylglycine whose subsequent Cu(I) catalysed alkyne–azide cycloaddition (CuAAC) with the corresponding alkylazides at the end of the synthesis is used to modulate their hydrophobic character.

Results and discussion

Synthesis of protected γ-amino acid 6

The synthesis of fully protected dihydroxylated-γ-amino acid **6** was carried out in five steps from commercially available (–)-shikimic acid (**1**), as outlined in Scheme 1. The key step was the simultaneous and diastereoselective reduction of the double bond and the azide group in compound **3**. First, the Mitsunobu reaction with previously reported protected shikimic acid, compound **2**,[32] by using freshly prepared hydrazoic acid[33] and diisopropyl azodicarboxylate (DIAD) as coupling reagent, afforded azide **3** in 76% yield. As mentioned above, simultaneous hydrogenolysis of the azide group and double

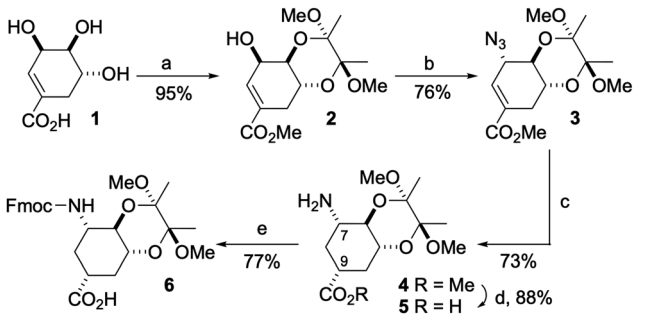

Scheme 1 Synthesis of protected γ-amino acid **6**. Reagents and conditions: (a) $(MeCO)_2$, $(MeO)_3CH$, H_2SO_4 (cat), MeOH, Δ. (b) HN_3, DIAD, Ph_3P, THF, 0 °C. (c) H_2, Pd/C (10%), MeOH, RT. (d) 1. LiOH (aq.), RT; 2. Amberlite CG-50 (H^+), RT. (e) Fmoc-Cl, Na_2CO_3, H_2O/acetone (2 : 1), 0 °C to RT.

bond reduction of **3** using palladium on carbon as a catalyst gave protected γ-amino ester **4** in 73% yield. The diastereoselectivity of the reaction was confirmed by NOE experiments (Fig. S1 and S2). Thus, inversion of the signal of H_9 led to enhancement of the signal of H_1 (0.3%), which confirmed the equatorial disposition of the carboxy methyl ester group. Basic hydrolysis of methyl ester **4** followed by protonation using Amberlite CG-50 (H^+) ion-exchange resin afforded γ-amino acid **5** in good yield. Finally, Fmoc-protection by treatment with 9-fluorenylmethoxycarbonyl chloride (Cl-Fmoc) in the presence of sodium carbonate gave the desired protected γ-amino acid **6** in 77% yield (Fig. S3).

Synthesis of cyclic peptides

The CPs reported here were synthesized using Fmoc-based solid phase peptide synthesis (Scheme 2).[34,35] Initially, Fmoc-D-Glu-OAll was anchored through its side chain to a Rink Amide resin.[36] Then, deprotection and coupling cycles were performed until the desired linear octapeptides were obtained. Next, the allyl and Fmoc groups at both ends were removed to carry out the cyclization on the solid support. The effectiveness of the cyclization was monitored after a period of 3 h by acidic cleavage (TFA/H_2O/TIS, 95 : 2.5 : 2.5) of a small portion of the resin (2–3 mg) and subsequent analysis by HPLC-MS. The alkyl chains were introduced by CuAAC reactions between the terminal alkyne groups in the solid supported CPs and the corresponding alkylazides.[17] Alkyl chains of ten and fourteen carbon atoms were selected considering our previous studies, in which CPs bearing these chains provided optimal pharmacological properties, combining high potency and selectivity with improved solubility.[17] Finally, the side chain deprotection and release of the CPs from the solid support were performed by treatment with a TFA cocktail. In most of the cases, the overall yield, after the corresponding HPLC purifications, ranged between 7 and 10%. No notable limitations were found in the cyclization step compared with all other α-D,L-CPs. Additionally, the **CP1** and **CP2** derivatives were also prepared following a similar strategy and obtained in comparable yields. All CPs were purified by RP-HPLC and obtained as the corresponding tris-trifluoroacetic salts with purities greater than 95%.

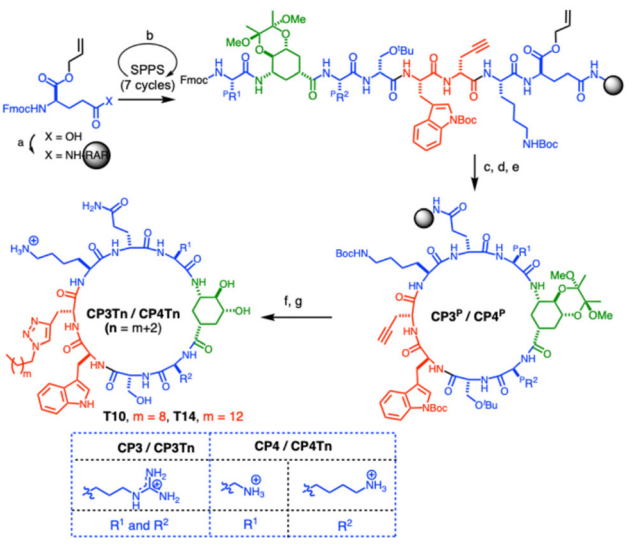

Scheme 2 Synthesis of cyclic peptides **CP3Tn** and **CP4Tn**. Reagents and conditions: (a) Rink amide resin (RAR), *N*-HBTU, DIEA, DMF; (b) SPPS: (i) piperidine/DMF (1 : 4); (ii) Fmoc-Aa-OH [by this order: Lys(Boc), D-Prg, Trp(Boc), D-Ser(^{t}Bu), Arg(Pbf)/Lys(Boc), **6**, Arg(Pbf)/Dap(Boc)], *N*-HBTU, DIEA, DMF; (c) piperidine/DMF (1 : 4); (d) $Pd(OAc)_2$, PPh_3, Ph_3SiH, NMM, DCM; (e) PyAOP, DIEA, DMF; (f) CuI, sodium ascorbate, DIEA, DMF; (g) TFA/H_2O/TIS (95 : 2.5 : 2.5). $^PR^1$ and $^PR^2$ denote the side chains of each residue with the corresponding protecting group.

Antibacterial activity and selectivity

To evaluate the efficacy of the cyclic peptides against pathogenic bacteria, the minimum inhibitory concentrations (MICs) were determined using the broth microdilution method in a 96-well plate.[37] MICs were obtained in triplicate experiments using aqueous stock solutions of the cyclic peptides (1 mg mL^{-1} in 0.9% NaCl) to provide two-fold serial dilution series ranging from 250 to 2 μg mL^{-1} and a final bug concentration in each well of 10^5 CFU mL^{-1}.[13,17] Three bacterial pathogens (two Gram-positive, *Staphylococcus aureus* (SA, ATCC 29213) and *Staphylococcus epidermidis* (SE, ATCC 12228), and one Gram-negative, *Escherichia coli* (EC, NCTC 10537)) were tested, and the results are summarized in Table 1. In general, CPs containing **Dhγ** show improved activities compared to their corresponding Ser-homologues. Therefore, the incorporation of the amino acid not only does not interfere with antibacterial activity but also improves it. As expected, the cyclic peptides proved to be more efficient against Gram-positive bacteria than Gram-negative (*E. coli*). Among the Gram-positive strains,

Table 1 Antimicrobial activities and cytotoxicity of the precursors and designed CPs

MIC [e] [μg mL^{-1}] (μM)				E_{max} [f] (%)	IC_{50} [g] (μM)
Peptide	SA [a]	SE [b]	EC [c]	NHDF-Neo [d]	
CP1	64 (47)	64 (47)	125–64	24 ± 8	—
CP2	250 (129.6)	125 (97.4)	>250	5 ± 4	—
CP3	250/125	32 (22.3)	>250	32 ± 2	—
CP4	>250	125	>250	29 ± 2	—
CP1T10	16 (10.9)	32 (21.8)	64 (41.2)	95 ± 1	39.8 ± 2.8
CP1T14	8 (5.0)	16 (10.0)	64 (40.0)	90 ± 1	26.9 ± 0.9
CP2T10	16 (10.8)	16 (10.8)	64	90 ± 1	45.0 ± 0.6
CP2T14	64 (41.6)	16 (10.4)	128	68 ± 1	21.7 ± 3.2
CP3T10	8 (4.9)	2 (1.2)	32 (19.7)	45 ± 1	—
CP3T14	16 (9.6)	16 (9.6)	64 (38)	70 ± 1	27.4 ± 1.6
CP4T10	8 (5.2)	4 (2.6)	125/64	25 ± 5	—
CP4T14	8 (5.0)	4 (2.5)	16 (10)	43 ± 3	—

[a] SA, *Staphylococcus aureus* (ATCC 29213). [b] SE, *Staphylococcus epidermidis* (ATCC 12228). [c] EC, *Escherichia coli* (NCTC 10537). [d] Human dermal fibroblasts (NHDF-Neo, CC-2509). [e] MICs in μmol L^{-1} (μM) are given in parentheses. [f] E_{max} is the maximum effect, which corresponds to the inhibition obtained at the highest concentration tested (100 μM). [g] IC_{50} is the concentration at which a 50% growth inhibition is obtained, and it was calculated only for those compounds with E_{max} values higher than 50%.

S. epidermidis is more susceptible to these CPs, being sensitive to almost all non-alkyl chain derivatives, except for **CP4**, which had moderate activity (125 μg mL^{-1}) against this strain. Although no major differences were identified between the different peptides, some minor variations were found that are worth mentioning. **CP4T10** is the peptide with the highest selectivity towards the Gram-positive bacteria, with negligible activity against *E. coli*. The most potent derivative was **CP3T10**, which achieved a MIC of 2 μg mL^{-1} (1.2 μM) against *S. epidermidis*. Among the **CP4** derivatives, no significant differences were observed in their activity against the Gram-positive strains. It should be noted that **CP4T14** has the broadest antibacterial spectrum, with MIC values ranging from 4 to 16 μg mL^{-1} (2.5 and 10 μM) against the Gram-positive bacteria and *E. coli*, respectively, confirming that longer alkyl chains tend to reduce the bacterial selectivity. Overall, the incorporation of **Dhγ** did not significantly modify the antibiotic activity compared to the corresponding Ser counterparts.

Cell viability in normal human dermal fibroblasts (NHDF-Neo, CC-2509) was determined by the MTT assay to assess the cytotoxicity of these CPs. The percentages of cell growth inhibition induced by increasing concentrations (from 0.78 μM to 100 μM) of the compounds were determined (Fig. S4 and Table 1).[38] Interestingly, most of the derivatives containing the **Dhγ** residue exhibited low cytotoxicity, with maximum response (E_{max}) values ranging between 25 and 70% at the highest tested concentration (100 μM). In general, and as we had initially proposed, the precursor derivatives containing Ser are more cytotoxic than those with the **Dhγ** residue, with the exception of **CP3T14** that exhibited an IC_{50} of 25 μM but is one of the less active CPs against the tested bacterial strains. Therefore, these results support, to some extent, the monosaccharide-mimetic behavior of this residue. In general, CPs lacking or having shorter alkyl chains were less cytotoxic compared to those with longer alkyl chains. This suggests that for derivatives with ten-carbon chains, initial electrostatic interactions must prevail over hydrophobic effects. In contrast, in the case of derivatives with longer alkyl chains, hydrophobic effects are likely to become predominant, broadening the spectrum of action and increasing cytotoxicity.[39,40] These results confirm that the observed selectivity is based, among other factors, on the combination of the initial electrostatic interactions with the anionic phospholipids, followed by the reorientation of the CPs/nanotubes to insert the alkyl tails into the hydrophobic core of the lipid bilayer. Based on previous studies,[41,42] it is most likely that these substructures subsequently cluster parallel to the membrane surface, leading to its disruption.

Supramolecular properties and nanotube formation

After confirming the antimicrobial properties and valuable contribution of **Dhγ** in reducing cytotoxicity in human cells thanks to the saccharide-like character it imparts to CPs, we proceeded to elucidate their self-assembling properties that support their behavior as supramolecular drugs. As mentioned above, our original proposal was based on the supramolecular capabilities of this class of D,L-α-CPs,[7] which self-assemble to form amphipathic nanotubes capable of disrupting bacterial membranes.[13–17] These supramolecular drugs[8,9] consist of low-toxicity monomers that are programmed to self-assemble into highly toxic membrane-active aggregates, in this particular case cationic amphipathic nanotubes. First, the self-assembling properties were evaluated under physiological conditions (10 mM PBS, 107 mM NaCl, pH 7.4) by using the thioflavin T (ThT) assay, which is a well-known method that gives a strong fluorescence emission upon binding to β-sheet rich structures.[43] Concentration-dependent experiments were carried out in the presence of ThT (20 μM). In all cases, a marked increase in fluorescence emission (494 nm) was observed as the concentrations of the CPs increased (Fig. 2a and S5). This emission was more pronounced for peptides with longer alkyl chains, whose critical aggregation concentration (cac) values at neutral pH were lower (Fig. 2b and S6). These results confirm that the formation of hydrogen bonds and the hydrophobic effects provided by the alkyl tail, which increase with the number of carbon atoms, drive the self-assembly and nanotube formation. The proximity of the cationic group (Dap *versus* Arg) to the nanotube backbone also plays an important role in modulating their assembly properties, increasing their cac (**CP4** analogues). Among the tested peptides, **CP3T14** exhibited the strongest self-assembling behavior, with the lowest cac value (25 μM). Therefore, the broad-spectrum activity of the CPs might be linked to the enhanced assem-

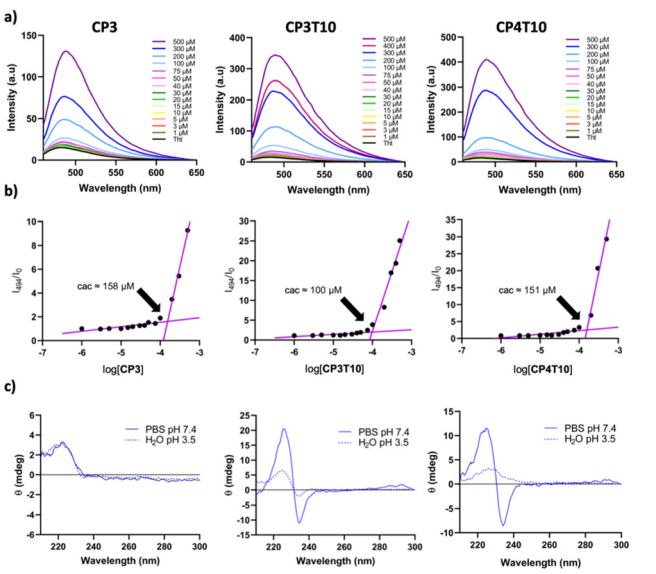

Fig. 2 (a) ThT fluorescence assays of **CP3**, **CP3T10** and **CP4T10** at different concentrations (1–500 μM) in PBS buffer (10 mM PBS, 107 mM NaCl) at pH 7.4. [ThT] = 20 μM, λ_{exc} = 440 nm. (b) Estimation of the cac using the dependence of I_{494}/I_0 on the sample concentration for **CP3**, **CP3T10** and **CP4T10** in PBS buffer (10 mM, 107 mM NaCl, pH 7.4). I_{494} is the ThT fluorescence emission intensity at 494 nm for samples containing CP and ThT, while I_0 is the fluorescence emission intensity at 494 nm of the ThT solution alone. (c) Overlaid far-UV CD spectra at 300 μM **CP3**, **CP3T10** and **CP4T10** in water solution at native pH (dashed line) and PBS buffer (10 mM, 107 mM NaCl, pH 7.4, bold line). The spectra were recorded using a 0.5 cm path length.

bling/hydrophobic properties of the derivatives bearing C14 alkyl chains. On the other hand, potency seems to improve with the incorporation of guanidinium groups (Arg), which not only exert a lower impact on stacking of CPs, but also interact more strongly with the phosphatidylserines present in bacterial membranes.[44]

The chiroptical properties induced by self-assembly and nanotube formation were also evaluated. To this end, CD experiments were performed to study the chirality of the supramolecular aggregates (Fig. 2c and S7). Measurements were carried out in water at pH ~ 3.5 and in PBS buffer (10 mM, 107 mM NaCl) at pH 7.4. **CP3** and **CP4** did not show clear evidence of supramolecular organization at any pH tested, as only a slightly positive band at 224 nm was observed. In contrast, the spectra of CP solutions with alkyl pendants displayed a stronger CD signal as the pH increased. While under acidic conditions the **CP3T*n*** derivatives already showed evidence of chiral supramolecular organization, the **CP4T*n*** derivatives, those incorporating 2,3-diaminopropionic acid instead of Arg, did not exhibit such organization under these conditions. Upon neutralization of the **CP4T10** solution, significant changes in its spectrum were observed with the identification of signals similar to those of **CP3T10** spectra that can be correlated with the corresponding structural changes. Specifically, at neutral pH (7.4), these peptides showed a positive band at 224 nm and a negative band at 235 nm, which can be attributed to Trp–peptide backbone interactions and the stacking of the indole group (Trp exciton-coupled bands).[17,45–47] This increase in the CD signal under physiological conditions suggests that the resulting nanotubes arrange Trp residues close to each other, probably due to the formation of parallel β-sheets between the CPs, which orient all the same residues aligned along the nanotube.[48,49] For **CP4**, the ammonium groups of the 2,3-diaminopropanoic residue aligned along the nanotube would be too close to each other and, consequently, their full protonation likely destabilize the supramolecular structure favouring its dissociation. Together with the ability of guanidinium cations to form like-charge ion pairs, this could explain the differences in assembly properties observed between **CP3T*n*** and **CP4T*n***. On the other hand, CPs lacking lipophilic chains can stack in both parallel and antiparallel β-sheets, while those with the alkyl side chains stack mainly in parallel sheets. The latter is due to the hydrophobic effects of these chains, which consequently determine the relative orientation of these residues and, therefore, the type of stacking of the CPs. Furthermore, the lack of the triazole and alkyl chain should confer greater conformational freedom to the indole moiety, resulting in the disappearance of the exciton-coupled band.

The β-sheet structure of the CPs was also studied by FTIR using lyophilised samples (Fig. S8).[50] In all cases, the presence of a network of hydrogen bonds, typical of strongly packed folded structures, was confirmed by the appearance of the characteristic amide A vibration band in the range of 3278–3285 cm^{-1}. Carbonyl vibration bands (amide I) at 1625–1630 cm^{-1} and a small shoulder around 1664–1678 cm^{-1} support the proposed parallel β-sheet structure.

Once the self-assembling properties guided by β-sheet type interactions of the CPs were confirmed, drop-casting of the solutions of the CPs (300 μM) at different pHs (7 and 9) over carbon-coated copper grids was analysed by STEM (Fig. 3a, b and S9). In most of the cases, sheet-like aggregates were observed,[51,52] although fibres were also detected. Most likely these 2D-structures are supramolecular assemblies formed by nanotube bilayers in which the Trp side chain and the alkyl pendants are arranged on the inner part of the bilayer to avoid contact with the water environment (Fig. 3c). This hierarchical organization leaves the hydrophilic residues exposed to the aqueous environment, covering the outer surface of these bilayers. The alkyl chanis are most likely intertwined and occupy the central part of the bilayer, which is located between the two outer faces of the membrane formed by the cyclic peptides. In addition, the di-equatorial diols of the γ-residues are also exposed to the external surface simulating an arrangement similar to that found in glucose or galactose moieties. These findings suggest that the hydrophobic effects are the main driving force behind the formation of the 2D materials, while lateral contacts between nanotubes must also play a key role in the formation of these structures, in which the **Dhγ** may also be supporting this aggregation. The dimensions of these 2D sheets were evaluated by atomic force microscopy

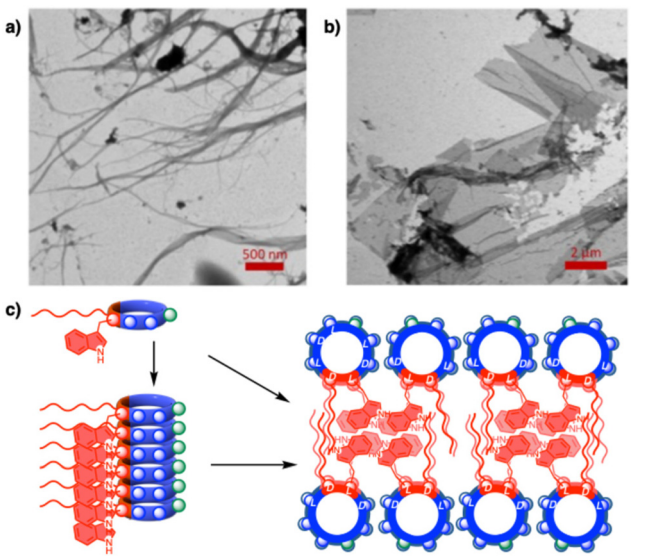

Fig. 3 (a) STEM micrograph of carbon-coated copper grids of **CP3** (300 μM) at pH 9.0. (b) STEM micrograph of carbon-coated copper grids of **CP3T10** (300 μM) at pH 7.0. (c) Hierarchical self-assembly of cyclic peptides to form nanotubes and two-dimensional sheets. The parallel stacking of CPs to form nanotubes, thanks to the network of hydrogen bonds characteristic of β-sheet-like structures between peptide bonds. Subsequent lateral aggregation guided by hydrophobic effects and π,π-stacking, together with interactions between the laterally associated nanotubes' side chains, drives the subsequent growth and formation of the two-dimensional structures. The red color represents hydrophobic residues, blue represents hydrophilic residues and green represents the dihydroxylated amino acids. This nanotube bilayer leaves at least one of the cationic residues (Arg/Dap) and the di-equatorial diols of the residues incorporated in this work exposed to the external environment.

(AFM) (Fig. S10). The deposition of an aqueous solution of **CP3T10** at neutral pH on the mica surface showed the presence of sheet-like structures with heights of 3.30 ± 0.22 nm. These values agree quite well with the lipid bilayer model proposed above. Most likely the alkyl chains are intertwined filling the internal space of the bilayer. The formation of such a structure confirms the cyclic peptide stacking to form supramolecular assemblies. These structures provide hydrophobic surfaces that further aggregate to form the 2D materials. Although we believe that this class of 2D materials is not directly involved in the mechanism of action of these CPs, these experiments confirmed the existence of lateral interactions between nanotubes that could be responsible for the formation of large aggregates on the bacterial membrane surface, resembling the "carpet-like" structures proposed in the mode of action of AMPs.

Conclusions

We have synthesized fully protected (1*R*,3*S*,4*R*,5*R*)-3-amino-4,5-dihydroxycyclohexane-1-carboxylic acid (**6**) from (–)-shikimic acid. This residue allows the design of a new class of nanotube-forming cyclic peptides, in which the hydroxyl groups are oriented outward on the surface of the nanotube, imparting carbohydrate-like characteristics.[29] To confirm this, the residue was incorporated into cationic amphipathic cyclic peptides that displayed strong antimicrobial activity against Gram-positive bacteria. Interestingly, derivatives containing this residue are also less cytotoxic in mammalian cell lines (fibroblasts) than those containing Ser, one of the naturally occurring residues bearing a single hydroxyl group. The characterization of these CPs provides strong evidence of their stacking properties to form nanotubes and their ability to continue to assemble into two-dimensional materials. In this lamellar structure, the hydrophobic side chains are shielded from the aqueous environment, forming a bilayer structure in which the alkyl chains and indole moieties are intertwined to create the central hydrophobic core of the bilayer, confirming the lateral hierarchical growth of these nanotubes. Based on this, the proposed mode of action resembles a carpet-like mechanism, in which the cyclic peptides accumulate on the anionic phospholipid-rich membranes. This high local concentration of CPs triggers hierarchical self-assembly, initially forming nanotubes that subsequently grow laterally, possibly forming large plaques on the membrane surface, leading to membrane destabilization and cell death. The supramolecular properties and antimicrobial activity of these CPs can be modulated by varying the length of the alkyl chain, the cationic character, and the nature of the linker of the residue located on the opposite side of the hydrophobic pendant group. The results obtained in this work suggest that membrane-active supramolecular drugs[8,9] could represent promising therapeutic tools for treating Gram-positive bacterial infections. This supramolecular approach may offer new alternatives that allow adaptation to the intrinsic properties of membranes. In this case, the antimicrobial efficacy of these CPs arises from a synergistic combination of electrostatic attraction with the anionic properties of the host membrane, the insertion of hydrophobic pendants into the membrane core, and hierarchical growth to form membrane-disrupting nanoplates. In addition, the use of simple dihydroxylated residues, such as (1*R*,3*S*,4*R*,5*R*)-3-amino-4,5-dihydroxy-cyclohexane-1-carboxylic acid, designed to resemble saccharide moieties, appears to provide some additional selectivity against mammalian cells.

Experimental

General

All starting materials and reagents were commercially available and were used without further purification. ^{1}H (250 and 500 MHz) and ^{13}C (63 MHz) spectra were recorded in deuterated solvents. *J* values are given in Hertz. NMR assignments were carried out using a combination of 1D, COSY, and DEPT-135 experiments. FTIR spectra were recorded for a powder sample in a PerkinElmer Spectrum Two ATR. $[\alpha]_D^{20}$ values are given in deg mL g^{-1} dm^{-1}. Melting points were measured using a Büchi M-560 apparatus. All procedures involving the use of ion-exchange resins were carried out at room temperature using Milli-Q deionized water.

Methyl (1*R*,3*S*,4*S*,6*R*,7*S*)-3,4-dimethyl-7-azido-3,4-dimethoxy-2,5-dioxabicyclo[4.4.0]dec-8-ene-9-carboxylate (3)

A stirred solution of alcohol **2**[32] (1 g, 3.31 mmol) in THF (30 mL) at 0 °C was treated successively with triphenylphosphine (1.32 g, 4.97 mmol), a freshly prepared solution of hydrazoic acid[33] in toluene (1.9 mL, 4.97 mmol) and finally diisopropyl azodicarboxylate (0.98 mL, 4.97 mmol) added dropwise. After stirring at room temperature for 1 h, the solvent was removed under reduced pressure and the resulting residue was purified by flash chromatography, eluting with (25 : 75) ethyl acetate/hexane, to yield azide **3** (825 mg, 76%) as a colorless oil. $[\alpha]_D^{20}$ = +37.4° (*c* 1.0, $CHCl_3$). ^{1}H NMR (250 MHz, $CDCl_3$) δ: 6.57 (t, *J* = 2.5 Hz, 1H, H2), 4.26 (m, 1H, H3), 3.87 (dd, *J* = 10.4 and 5.6 Hz, 1H, H5), 3.79 (m, 1H, H4), 3.75 (s, 3H, OCH_3), 3.34 (s, 3H, OCH_3), 3.27 (s, 3H, OCH_3), 2.74 (m, 1H, C*H*H-6), 2.31 (m, 1H, CH*H*-6), 1.35 (s, 3H, CH_3) and 1.32 (s, 3H, CH_3) ppm. ^{13}C NMR (63 MHz, $CDCl_3$) δ: 166.1 (C), 134.6 (CH), 130.6 (C), 99.9 (C), 99.5 (C), 72.8 (CH), 65.8 (CH), 60.6 (CH), 52.3 (OCH_3), 48.3 (OCH_3), 48.2 (OCH_3), 29.4 (CH_2) and 17.8 (2 × CH_3) ppm. FTIR (film) ν = 2100 (N≡N) and 1714 (CO) cm^{-1}. MS (ESI) *m*/*z* = 350 (MNa^+). HRMS calcd for $C_{14}H_{21}N_3O_6Na$ (MNa^+): 350.1323; found, 350.1314.

Methyl (1*R*,3*S*,4*S*,6*R*,7*R*,9*R*)-7-amino-3,4-dimethyl-3,4-dimethoxy-2,5-dioxabicyclo[4.4.0]decane-9-carboxylate (4)

To a stirred suspension of 10% palladium on carbon (35 mg) in methanol (5.5 mL) under a hydrogen atmosphere, a solution of azide **3** (355 mg, 1.09 mmol) in methanol (5.5 mL) was added *via* cannula. The resulting suspension was stirred at room temperature for 18 h. The hydrogen atmosphere was

removed under vacuum and the suspension was filtered through a plug of Celite®. The filtrates and the washings (methanol) were concentrated under reduced pressure. The residue that resulted was purified by flash chromatography, eluting with (10 : 90) methanol/dichloromethane, to afford amine **4** (220 mg, 73%) as a colorless oil. $[\alpha]_D^{20}$ = +161.1° (*c* 4.3, $CHCl_3$). ^{1}H NMR (500 MHz, $CDCl_3$) δ: 3.69 (s, 3H, OCH_3), 3.66 (td, *J* = 9.9 and 4.4 Hz, 1H, H1), 3.36 (t, *J* = 9.9 Hz, 1H, H6), 3.31 (s, 3H, OCH_3), 3.25 (s, 3H, OCH_3), 3.08 (m, 1H, H7), 2.86 (m, 1H, H9), 2.43 (m, 1H, C*H*H), 2.29 (m, 1H, CH*H*), 1.65 (dt, *J* = 12.7 and 5.2 Hz, 1H, C*H*H), 1.59 (dt, *J* = 12.4 and 4.8 Hz, 1H, CH*H*), 1.33 (s, 3H, CH_3) and 1.30 (s, 3H, CH_3) ppm. ^{13}C NMR (63 MHz, $CDCl_3$) δ: 174.2 (C), 99.6 (2 × C), 76.8 (CH), 68.4 (OCH_3), 52.0 (CH), 50.7 (CH), 48.0 (OCH_3), 47.9 (OCH_3), 39.1 (CH), 35.4 (CH_2), 31.9 (CH_2) and 17.8 (2 × CH_3) ppm. FTIR (film) ν: 3583 (NH) and 1734 (CO) cm^{-1}. MS (ESI) *m*/*z* = 304 (MH^+). HRMS calcd for $C_{14}H_{26}NO_6$ (MH^+): 304.1755; found, 304.1758.

(1*R*,3*S*,4*S*,6*R*,7*R*,9*R*)-7-Amino-3,4-dimethyl-3,4-dimethoxy-2,5-dioxabicyclo[4.4.0]decane-9-carboxylic acid (5)

A solution of ester **4** (28 mg, 0.09 mmol) in THF (0.9 mL) at room temperature was treated with an aqueous solution of LiOH (0.5 mL, 0.25 mmol, 0.5 M). After stirring for 30 min, water was added and THF was removed under reduced pressure. The aqueous layer was washed with diethyl ether (×3) and then treated with Amberlite CG-50 (H^+) until pH 6. The resin was filtered off and washed with Milli-Q water. The filtrate and the washings were lyophilized to afford acid **5** (23 mg, 88%) as a colorless oil. $[\alpha]_D^{20}$ = +189.8° (*c*1.0, $CDCl_3$). ^{1}H NMR (250 MHz, $CDCl_3$) δ: 7.63 (br s, 1H, NH), 3.63–3.42 (m, 2H, H6 + H1), 3.23 (m, 1H, H7), 3.19 (s, 6H, 2 × OCH_3), 2.34 (m, 1H, H9), 2.18 (m, 1H, C*H*H), 2.00 (m, 1H, CH*H*), 1.60–1.35 (m, 2H, CH_2), 1.25 (s, 3H, CH_3) and 1.23 (s, 3H, CH_3) ppm. ^{13}C NMR (63 MHz, $CDCl_3$) δ: 183.4 (C), 102.7 (C), 102.6 (C), 74.4 (CH), 70.9 (CH), 52.4 (CH), 50.5 (OCH_3), 50.3 (OCH_3), 43.5 (CH), 34.1 (CH_2), 33.9 (CH_2) and 19.3 (2 × CH_3) ppm. FTIR (film) ν = 3435 (NH) and 1673 (CO) cm^{-1}. MS (ESI) *m*/*z* = 288 (M − H). HRMS calcd for $C_{13}H_{22}NO_6$ (M − H): 288.1453; found, 288.1447.

(1*R*,3*S*,4*S*,6*R*,7*S*,9*R*)-7-(((9*H*-Fluoren-9-yl)methoxy)carbonyl) amino-3,4-dimethyl-3,4-dimethoxy-2,5-dioxabicyclo[4.4.0] decane-9-carboxylic acid (6)

A stirred solution of amine **5** (50 mg, 0.17 mmol) and sodium carbonate (55 mg, 0.52 mmol) in a (2 : 1) mixture of acetone/water (2.1 mL) at 0 °C was treated dropwise with a solution of 9-fluorenyl chloroformate (49.2 mg, 0.19 mmol) in acetone (0.8 mL). The reaction mixture was stirred at room temperature for 10 h and then heated at 50 °C for 2 h. After cooling to room temperature, the reaction mixture was extracted with diethyl ether. The aqueous phase was acidified with HCl (10%) until pH 5 and then extracted with ethyl acetate (×3). The combined organic extracts were dried (Na_2SO_4 anh.), filtered and concentrated under reduced pressure. The resulting residue was purified by flash chromatography, eluting with (10 : 90) methanol/dichloromethane, to afford Fmoc-protected amino acid **6** (61 mg, 71%) as a white solid. Mp: 113–114 °C. $[\alpha]_D^{20}$ = +67.7° (*c* 2.9, $CHCl_3$). ^{1}H NMR (250 MHz, DMSO-d_6) δ: 7.88 (d, *J* = 7.5 Hz, 2H, 2 × ArH), 7.68 (d, *J* = 7.4 Hz, 2H, 2 × ArH), 7.41 (t, *J* = 7.3 Hz, 2H, 2 × ArH), 7.30 (t, *J* = 7.4 Hz, 2H, 2 × ArH), 4.32 (m, 1H, CH-9′), 4.24 (d, *J* = 6.8 Hz, 2H, OCH_2), 3.49 (m, 2H, H7 + H1), 3.29 (d, *J* = 9.6 Hz, 2H, H6), 3.13 (s, 6H, 2 × OCH_3), 1.88 (m, 1H, H9), 1.51–1.22 (m, 4H, 2 × CH_2), 1.15 (s, 3H, CH_3) and 1.12 (s, 3H, CH_3) ppm. ^{13}C NMR (63 MHz, DMSO-d_6) δ: 175.3 (C), 155.7 (C), 144.0 (2 × C), 140.7 (2 × C), 127.6 (2 × CH), 127.0 (2 × CH), 125.1 (2 × CH), 120.1 (2 × CH), 98.9 (C), 98.8 (C), 72.7 (CH), 68.4 (CH), 65.2 (CH_2), 49.8 (CH), 47.3 (2 × OCH_3), 46.7 (CH), 38.2 (CH), 33.9 (CH_2), 31.7 (CH_2), 17.7 (CH_3) and 17.6 (CH_3) ppm. IR (KBr) ν = 3437 (NH) and 1693 (CO) cm^{-1}. MS (ESI) *m*/*z* = 534 (MNa^+). HRMS calcd for $C_{28}H_{33}NO_8Na$ (MNa^+): 534.2098; found, 534.2091.

Synthesis of cyclic peptides

For detailed descriptions of the preparation methods of cyclic peptide derivatives and precursors, see the SI. All CPs, after the corresponding solid phase synthesis, were purified by RP-HPLC and were obtained with purities greater than 95%.

Antibacterial activity assays

The bacterial strains used in these assays were *Staphylococcus aureus* (SA, ATCC 29213), *Staphylococcus epidermidis* (SE, ATCC 12228) and *Escherichia coli* (EC, NCTC 10537). The bacterial strains were grown the day before at 37 °C in Brain–Heart Agar plates (Scharlab, S.L. Barcelona, Spain). Then, the selected colonies were incubated in Mueller–Hinton Broth (MHB) (Scharlab, S.L. Barcelona, Spain) at 35 °C for 1 h and adjusted to 0.5 McFarland units. Then, a bacterial suspension (~10^6 CFU mL^{-1}) in Mueller–Hinton Broth was prepared. The concentrations of these initial bacterial suspensions were regularly tested by CFU counting. The peptide solutions (from 250 to 2 μg mL^{-1}) were made directly in 96-well plates containing Mueller–Hinton Broth, starting from a peptide stock solution at a concentration of 1 mg mL^{-1} in an aqueous solution of NaCl (0.9%). Next, 10 μL per well of bacterial suspension was added. The final volume per well was 100 μL at a bacterial concentration of 10^5 CFU mL^{-1}. The samples were incubated for 24 h at 37 °C. Then, the optical density (OD) at 620 nm was measured using a Biochrom EZ Read 400 ELISA microplate reader with Galapagos software. The data were normalized to the value of untreated bacterial suspensions (growth control) and all experiments were performed in triplicate. The minimal inhibitory concentration (MIC) was calculated as the lowest concentration at which complete inhibition of bacterial growth was observed.

MTT assay in human dermal fibroblasts

NHDF-Neo (CC-2509) cells were cultured at 100 000 cells per mL in 96-well plates (100 μL per well) for 24 hours in an atmosphere of 95% air and 5% CO_2 at 37 °C. The medium was supplemented with 10% FBS (fetal bovine serum) and 1% penicillin–streptomycin–glutamine mixture. The cyclic peptides were

dissolved in Milli-Q H_2O and diluted to the desired concentration with complete medium. The water content was maintained at less than 1%. Then, the cells were incubated with the cyclic peptide solutions (100 μL per well). After 72 hours, the samples were removed and 100 μL of complete medium with 0.5 mg ml^{-1} MTT were added to each well.[53,54] The cells were incubated for 4 hours, and the medium was removed. The resulting formazan crystals were dissolved in DMSO (100 μL per well). The absorbance of each well at 570 nm was acquired with a Tecan Infinite F200 Pro plate reader. A blank subtraction was performed (cells treated with Triton X-100) and the data were normalized to the value of the untreated cells (100% viability). Data were analysed with GraphPad Prism software.[55]

ThT fluorescence assay

Thioflavin T (ThT)[43] fluorescence experiments were performed using a Varian Cary Eclipse spectrophotometer equipped with a temperature-controlled cell chamber. Spectra were recorded at 20 °C in a Hellma® fluorescence quartz cuvette (10 mm × 4 mm), using an excitation wavelength of 440 nm. Samples containing ThT (20 μM) and the corresponding peptide in the specified concentration range and buffer were prepared. The resulting solutions were allowed to equilibrate for 30 minutes before measuring fluorescence.

Circular dichroism

Circular dichroism (CD) measurements were acquired in a Jasco J-1100 CD spectrometer equipped with a Jasco MCB-100 mini circulation bath for controlling the temperature. Measurements were carried out in a 0.5 cm quartz cuvette at 20 °C and the specified pH and concentration. The equipment was configured for 100 nm min^{-1} scanning speed, 1 second response time, 1 nm bandwidth and 0.2 nm data pitch. Each spectrum corresponds to the average of 10 scans, and the solvent background was corrected.

Scanning transmission electron microscopy (STEM)

STEM images were obtained using a ZEISS FESEM ULTRA Plus with EDX operating at a high voltage of 20 kV. Samples were prepared by deposition of a peptide solution (300 μM, 10 μL) at the specified pH over a 400-mesh carbon-coated copper grid (Electron Microscopy Sciences). After 10 minutes, the excess sample was removed with a filter paper. Then, the samples were stained with an aqueous solution of phosphotungstic acid (2% w/v, 10 μL) for 3 minutes and washed with Milli-Q H_2O (10 μL) for 1 minute. The samples were allowed to air-dry overnight before imaging.

Atomic force microscopy (AFM)

Atomic force microscopy measurements were performed at room temperature and ambient atmosphere using a Park Systems XE-100 in non-contact mode. ACTA tips were used (silicon tips, nominal values: spring constant = 40 N m^{-1}, frequency = 300 kHz, ROC less than 10 nm). Briefly, 10 μL of CP aqueous solutions at the specified pH and concentration were added dropwise onto a mica substrate. After 5 min, the sample was thoroughly washed with Milli-Q-H_2O and dried under an argon flow. Image analysis was carried out with Gwyddion.[56]

Author contributions

E. G.-F.: synthesis of the cyclic peptides and antimicrobial evaluation. M. V.-P.: nanotube characterization and cytotoxicity studies. V. P.: synthesis of the protected γ-amino acid. R. S. and A. P.-E.: antimicrobial evaluation. M. A., C. G.-B. and J. R. G.: design and evaluation of results. C. G.-B., M. V.-P. and J. R. G.: writing.

Conflicts of interest

There are no conflicts to declare.

Data availability

All supporting data are provided in the supplementary information (SI). This includes figures of NMR spectra of amino acid synthesis intermediates and cyclic peptides, cell viability graphs, CAC determination and fluorescence studies, CD and FTIR spectra, STEM and AFM Pictures. There is also a description of the solid-phase synthesis protocol for preparing cyclic peptides. See DOI: **https://doi.org/10.1039/d5qo01374g**.

Acknowledgements

This work was funded by the Spanish State Agency of Research (PID2022-142440NB-I00, SAF2013-42899-R, PID2022-136963OB-I00), the Xunta de Galicia (ED431C 2021/21, ED431C 2025/15, ED431C 2025/05 and Centro singular de investigación de Galicia accreditation 2023-2027, ED431G 2023/03), and the European Regional Development Fund (ERDF). E. G.-F. thanks the Xunta de Galicia for her research contract (ED481A-2019/117). V. P. thanks the Spanish Ministry of Economy and Competitiveness for her FPI fellowship (BES-2011-047452). M. V.-P. thanks the Spanish Ministry of Universities for his FPU contract.

References

1 R. E. Baker, A. S. Mahmud, I. F. Miller, M. Rajeev, F. Rasambainarivo, B. L. Rice, S. Takahashi, A. J. Tatem, C. E. Wagner, L.-F. Wang, A. Wesolowski and C. J. E. Metcalf, Infectious disease in an era of global change, *Nat. Rev. Microbiol.*, 2022, **20**, 193–205.
2 R. Tommasi, D. G. Brown, G. K. Walkup, J. I. Manchester and A. A. Miller, ESKAPEing the labyrinth of antibacterial Discovery, *Nat. Rev. Drug Discovery*, 2015, **14**, 529–542.

3 V. M. D'Costa, C. E. King, L. Kalan, M. Morar, W. W. Sung, C. Schwarz, D. Froese, G. Zazula, F. Calmels, R. Debruyne, G. B. Golding, H. N. Poinar and G. D. Wright, Antibiotic resistance is ancient, *Nature*, 2011, **477**, 457–461.
4 **https://www.who.int/news-room/fact-sheets/detail/antimicrobial-resistance**.
5 N. Mookherjee, M. A. Anderson, H. P. Haagsman and D. J. Davidson, Antimicrobial host defence peptides: functions and clinical potential, *Nat. Rev. Drug Discovery*, 2020, **19**, 311–332.
6 M. Abdi, S. Mirkalantari and N. Amirmozafari, Bacterial resistance to antimicrobial peptides, *J. Pept. Sci.*, 2019, **25**, e3210.
7 N. Rodríguez-Vázquez, H. L. Ozores, A. Guerra, E. González-Freire, A. Fuertes, M. Panciera, J. M. Priegue, J. Outeiral, J. Montenegro, R. García-Fandino, M. Amorín and J. R. Granja, Membrane-targeted self-assembling cyclic peptide nanotubes, *Curr. Top. Med. Chem.*, 2014, **14**, 2647–2661.
8 K. Kawakami, M. Ebara, H. Izawa, N. M. Sanchez-Ballester, J. P. Hill and K. Ariga, Supramolecular approaches for drug development, *Curr. Med. Chem.*, 2012, **19**, 2388–2398.
9 S. L. Regen, Drug discovery and the supramolecular factor, *ACS Med. Chem. Lett.*, 2023, **14**, 687–688.
10 D. T. Bong, T. D. Clark, J. R. Granja and M. R. Ghadiri, Self-assembling organic nanotubes, *Angew. Chem., Int. Ed.*, 2001, **40**, 988–1011.
11 N. Rodríguez-Vázquez, M. Amorín and J. R. Granja, Recent advances in controlling the internal and external properties of self-assembling cyclic peptide nanotubes and dimers, *Org. Biomol. Chem.*, 2017, **15**, 4490–4505.
12 Q. Song, Z. Cheng, M. Kariuki, S. C. L. Hall, S. K. Hill, J. Y. Rho and S. Perrier, Molecular self-assembly and supramolecular chemistry of cyclic peptides, *Chem. Rev.*, 2021, **121**, 13936–13995.
13 S. Fernández-Lopez, H.-S. Kim, E. C. Choi, M. Delgado, J. R. Granja, A. Khasanov, K. Kraehenbuehl, G. Long, D. A. Weinberger, K. M. Wilcoxen and M. R. Ghadiri, Antibacterial agents based on the cyclic D,L-α-peptide architecture, *Nature*, 2001, **412**, 452–455.
14 V. Dartois, J. Sanchez-Quesada, E. Cabezas, E. Chi, C. Dubbelde, C. Dunn, J. R. Granja, C. Gritzen, D. Weinberger, M. R. Ghadiri and T. R. Parr, Systemic antibacterial activity of novel synthetic cyclic peptides, *Antimicrob. Agents Chemother.*, 2005, **49**, 3302–3310.
15 M. Hartlieb, S. Catrouillet, A. Kuroki, C. Sanchez-Cano, R. Peltier and S. Perrier, Stimuli-responsive membrane activity of cyclic-peptide–polymer conjugates, *Chem. Sci.*, 2019, **10**, 5476–5483.
16 P. B. Chen, A. S. Black, A. L. Sobel, Y. Zhao, P. Mukherjee, B. Molparia, N. E. Moore, G. R. A. Muench, J. Wu, W. Chen, A. F. M. Pinto, B. E. Maryanoff, A. Saghatelian, P. Soroosh, A. Torkamani, L. J. Leman and M. R. Ghadiri, Directed remodeling of the mouse gut microbiome inhibits the development of atherosclerosis, *Nat. Biotechnol.*, 2020, **38**, 1288–1297.
17 E. González-Freire, F. Novelli, A. Pérez-Estrada, R. Seoane, M. Amorín and J. R. Granja, Double orthogonal click reactions for the development of antimicrobial peptide nanotubes, *Chem. – Eur. J.*, 2011, **27**, 3029–3038.
18 L. Motiei, S. Rahimipour, D. A. Thayer, C.-H. Wong and M. R. Ghadiri, Antibacterial cyclic D,L-α-glycopeptides, *Chem. Commun.*, 2009, 3693–3695.
19 A. Pizzi, L. H. Ozores, M. Calvelo, R. García-Fandiño, M. Amorín, N. Demitri, G. Terraneo, S. Bracco, A. Comotti, P. Sozzani, C. X. Bezuidenhout, P. Metrangolo and J. R. Granja, Tight xenon confinement in a crystalline sandwich-like hydrogen-bonded dimeric capsule of a cyclic peptide, *Angew. Chem., Int. Ed.*, 2019, **58**, 14472–11447.
20 H. L. Ozores, M. Amorín and J. R. Granja, Self-assembling molecular capsules based on α,γ-cyclic peptides, *J. Am. Chem. Soc.*, 2017, **139**, 776–784.
21 A. Fuertes, H. L. Ozores, M. Amorín and J. R. Granja, Self-assembling Venturi-like peptide nanotubes, *Nanoscale*, 2017, **9**, 748–753.
22 M. Amorín, L. Castedo and J. R. Granja, New cyclic peptide assemblies with hydrophobic cavities: the structural and thermodynamic basis of a new class of peptide nanotubes, *J. Am. Chem. Soc.*, 2003, **125**, 2844–2845.
23 R. J. Brea, M. Amorín, L. Castedo and J. R. Granja, Methyl-blocked dimeric α,γ-peptide nanotube segments: formation of a peptide heterodimer through backbone–backbone interactions, *Angew. Chem., Int. Ed.*, 2005, **44**, 5710–5713.
24 N. Rodríguez-Vázquez, M. Amorín, I. Alfonso and J. R. Granja, Anion recognition and induced self-assembly of an α,γ-cyclic peptide to form spherical clusters, *Angew. Chem., Int. Ed.*, 2016, **55**, 4504–4508.
25 N. Rodríguez-Vázquez, R. García-Fandiño, M. Amorín and J. R. Granja, Self-assembling α,γ-cyclic peptides that generate cavities with tunable properties, *Chem. Sci.*, 2016, **7**, 183–187.
26 M. Amorín, L. Castedo and J. R. Granja, Folding control in cyclic peptides through N-methylation pattern selection: formation of antiparallel β-sheet dimers, double reverse turns and supramolecular helices by 3α,γ cyclic peptides, *Chem. – Eur. J.*, 2008, **14**, 2100–2111.
27 N. Rodríguez-Vázquez, S. Salzinger, L. F. Silva, M. Amorín and J. R. Granja, Synthesis of cyclic γ-amino acids for foldamers and peptide nanotubes, *Eur. J. Org. Chem.*, 2013, 3477–3493.
28 A. Guerra, R. J. Brea, M. Amorín, L. Castedo and J. R. Granja, Self-assembling properties of all γ-cyclic peptides containing sugar amino acid residues, *Org. Biomol. Chem.*, 2012, **10**, 8762–8766.
29 S. A. W. Gruner, E. Locardi, E. Lohof and H. Kessler, Carbohydrate-based mimetics in drug design: sugar amino acids and carbohydrate scaffolds, *Chem. Rev.*, 2002, **102**, 491–514.
30 A. K. Bose, B. K. Banik, C. Mathur, D. R. Wagle and M. S. Manhas, Polyhydroxy amino acid derivatives via β-lactams using enantiospecific approaches and microwave techniques, *Tetrahedron*, 2000, **56**, 5603–5619.

31 Because of the chirality of amino acid **6**, **CP1** and **CP2** used as models for the cyclic peptide design are the enantiomers of the originally prepared CPs. In this way, the L-Ser, labelled in green, can be replaced with **DHγ** without altering the ability to adopt the required flat conformation. In any case, precedent studies with this class of peptides have already shown that in most cases both enantiomers α-D,L-CPs have similar activity.[13].

32 B. Blanco, V. Prado, L. Emilio, J. M. Otero, C. García-Doval, M. J. van Raaij, A. L. Llamas-Saiz, H. Lamb, A. R. Hawkins and C. González-Bello, *Mycobacterium tuberculosis* shikimate kinase inhibitors, *J. Am. Chem. Soc.*, 2013, **135**, 12366–12376.

33 M. Marchini, M. Mingozzi, R. Colombo, I. Guzzetti, L. Belvisi, F. Vasile, D. Potenza, U. Piarulli, D. Arosio and C. Gennari, Cyclic RGD peptidomimetics containing bifunctional diketopiperazine scaffolds as new potent integrin ligands, *Chem. – Eur. J.*, 2012, **18**, 6195–6207.

34 J. M. Palomo, Solid-phase peptide synthesis: an overview focused on the preparation of biologically relevant peptides, *RSC Adv.*, 2014, **4**, 32658–32672.

35 L. A. Carpino and G. Y. Han, 9-Fluorenylmethoxycarbonyl function, a new base-sensitive amino-protecting group, *J. Am. Chem. Soc.*, 1970, **92**, 5748–5749.

36 P. Rovero, L. Quartara and G. Fabbri, Synthesis of cyclic peptides on solid support, *Tetrahedron Lett.*, 1991, **32**, 2639–2642.

37 I. Wiegand, K. Hilpert and R. Hancock, Agar and broth dilution methods to determine the minimal inhibitory concentration (MIC) of antimicrobial substances, *Nat. Protoc.*, 2008, **3**, 163–175.

38 J. van Meerloo, G. J. L. Kaspers and J. Cloos, Cell Sensitivity Assays: The MTT Assay, in *Cancer Cell Culture. Methods in Molecular Biology*, ed. I. Cree, Humana Press, 2011, vol. 731.

39 A. Cabezón, M. Calvelo, J. R. Granja, Á. Piñeiro and R. Garcia-Fandino, Uncovering the mechanisms of cyclic peptide self-assembly in membranes with the chirality-aware MA(R/S)TINI forcefield, *J. Colloid Interface Sci.*, 2023, **642**, 84–99.

40 B. Claro, E. González-Freire, M. Calvelo, L. J. Bessa, E. Goormaghtigh, M. Amorín, J. R. Granja, R. Garcia-Fandiño, J. Gallová, D. Uhríková, A. Fedorov, A. Coutinho and M. Bastos, Membrane targeting antimicrobial cyclic peptide nanotubes – an experimental and computational study, *Colloids Surf., B*, 2020, **196**, 111349.

41 B. Claro, A. Peón, E. González-Freire, E. Goormaghtigh, M. Amorín, J. R. Granja, R. Garcia-Fandiño and M. Bastos, Macromolecular assembly and membrane activity of antimicrobial d,l-α-cyclic peptides, *Colloids Surf., B*, 2021, **208**, 112086.

42 B. Claro, E. González-Freire, J. R. Granja, R. Garcia-Fandiño, J. Gallová, D. Uhríková, A. Fedorov, A. Coutinho and M. Bastos, Partition of antimicrobial D,L-α-cyclic peptides into bacterial model membranes, *Biochim. Biophys. Acta, Biomembr.*, 2022, **1864**, 183729.

43 M. Biancalana, K. Makabe, A. Koide and S. Koide, Molecular mechanism of thioflavin-T binding to the surface of β-rich peptide self-assemblies, *J. Mol. Biol.*, 2009, **385**, 1052–1063.

44 L. Li, I. Vorobyov and T. W. Allen, The different interactions of lysine and arginine side chains with lipid membranas, *J. Phys. Chem. B*, 2013, **117**, 11906–11920.

45 A. G. Cochran, N. J. Skelton and M. A. Starovasnik, Tryptophan zippers: Stable, monomeric β-hairpins, *Proc. Natl. Acad. Sci. U. S. A.*, 2001, **98**, 5578–5583.

46 I. B. Grishina and R. W. Woody, Contributions of tryptophan side chains to the circular dichroism of globular proteins: exciton couplets and coupled oscillators, *Faraday Discuss.*, 1994, **99**, 245–262.

47 R. W. Woody, Contributions of tryptophan side chains to the far-ultraviolet circular dichroism of proteins, *Eur. Biophys. J.*, 1994, **23**, 253–262.

48 M. Calvelo, A. Lamas, A. Guerra, M. Amorín, R. García-Fandiño and J. R. Granja, Parallel versus antiparallel β-sheet structure in cyclic peptide hybrids containing γ- or δ-cyclic amino acids, *Chem. – Eur. J.*, 2020, **26**, 5846–5858.

49 M. R. Silk, J. Newman, J. C. Ratcliffe, J. F. White, T. Caradoc-Davies, J. R. Price, S. X. B. Perrier, P. E. Thompson and D. K. Chalmers, Parallel and antiparallel cyclic D/L peptide nanotubes, *Chem. Commun.*, 2017, **53**, 6613–6616.

50 S. Krimm and J. Bandekar, Vibrational spectroscopy and conformation of peptides, polypeptides, and proteins, *Adv. Protein Chem.*, 1986, **38**, 181–364.

51 I. Insua and J. Montenegro, 1D to 2D self assembly of cyclic peptides, *J. Am. Chem. Soc.*, 2020, **142**, 300–307.

52 S. Díaz, I. Insua, G. Bhak and J. Montenegro, Sequence decoding of 1D to 2D self-assembling cyclic peptides, *Chem. – Eur. J.*, 2020, **26**, 14765–14770.

53 T. Mossman, Rapid colorimetric assay for cellular growth and survival: application to proliferation and cytotoxicity assays, *J. Immunol. Methods*, 1983, **65**, 55–63.

54 P. Kumar, A. Nagarajan and P. D. Uchil, Analysis of cell viability by the MTT assay, *Cold Spring Harb. Protoc.*, 2018, 469–471.

55 M. L. Swift, GraphPad prism, data analysis, and scientific graphing, *J. Chem. Inf. Comput. Sci.*, 1997, **37**, 411–412.

56 D. Nečas and P. Klapetek, Gwyddion: an open-source software for SPM data analysis, *Cent. Eur. J. Phys.*, 2012, **10**, 181–188.

